

FABRICATION AND CHARACTERIZATIONS OF ZIRCONIUM BASED HIGH K DIELECTRIC THIN FILM BY WET CHEMICAL METHOD

A thesis Submitted in partial fulfilment of the requirement

For the degree of

Master of Science in physics

By

Neeha Pradhani

Roll No.:412ph2108

Under the supervision of

Dr. JyotiPrakashKar



**Department of Physics and Astronomy
National Institute of Technology
Rourkela-769008
Odisha, India**

Department of Physics and Astronomy



National Institute of Technology, Rourkela

Rourkela – 769008, Orissa, India

CERTIFICATE

This to certify that, the work in the report entitled “*FABRICATION AND CHARACTERIZATIONS OF ZIRCONIUM BASED HIGH K DIELECTRIC THIN FILM BY WET CHEMICAL METHOD*” by ***Miss Neeha Pradhani***, in partial fulfillment of Master of Science degree in PHYSICS at the National Institute of Technology, Rourkela; is an authentic work carried out by her under my supervision and guidance. The work is satisfactory to the best my knowledge.

Dr. Jyoti Prakash Kar

Department of Physics and Astronomy

National Institute of Technology

Rourkela-769008

ACKNOWLEDGEMENT

I have taken effort in this project entitled “FABRICATION AND CHARACTERIZATIONS OF ZIRCONIUM BASED HIGH K DIELECTRIC THIN FILM BY WET CHEMICAL METHOD”. It would not have been very difficult for me to complete this project without the kind support. I would like to thank all of them who helped me in this project work. I thank to my Guide, Dr. J.P Kar, Professor in Physics and Astronomy, NIT Rourkela for his continuous thoughtful discussion during the course of present work. I am very grateful to him.

I would like to thank to our research scholar, Mr. Kailash Chandra Dash, Mr. Surya Prakash Ghosh and Mr. Nilakantha Tripathy for giving me such attention and time and lastly I would like to express my heartfelt thanks to my beloved parents for their blessing.

Date:

Neeha Pradhani

TABLE OF CONTENTS

List of Figures.....	v
Chapter 1: Introduction.....	1
1.1: Why High K Dielectrics.....	1
1.2: Motivation for Zirconium Oxide.....	2
1.3: Zirconium Oxide material properties.....	3
1.4: Metal Oxide Semiconductor Structure (MOS Structure).....	4
Chapter 2: Fabrication Technology of Zirconium Oxide Thin film	5
2.1: Spin coating.....	5
2.2: Thermal evaporation.....	6
2.3: Experimental work.....	6
Chapter 3: Characterization Techniques	9
3.1: X-ray diffraction (XRD).....	9
3.2: Field emission scanning electron microscope(FESEM).....	10
3.3: UV-Visible Spectroscopy	11
3.4: Fourier transform infrared spectroscopy.....	12
3.5: Capacitance -Voltage measurement (C-V measurement).....	12
Chapter 4:Results and Discussion.....	16
4.1: X-Ray diffraction (XRD).....	16
4.2: .Field Emission Scanning Electron Microscope(FESEM).....	17
4.3.Fourier Transform Infrared Spectroscopy.....	17
4.4: UV-Visible Spectroscopy	18
4.5: Capacitance -Voltage measurement (C-V measurement).....	20
Chapter 5: Conclusion	21
Reference.....	22

LIST OF FIGURES

Figure 1.4 Cross-sectional view of a MOS structure.....	4
Figure 2.1 Steps of spin coating methods.....	6
Figure 2.2 Block diagram of thermal evaporation system.....	6
Figure 3.1 X-Ray Diffraction condition.....	9
Figure 3.2(a) The emission of secondary Electrons from the specimen.....	10
Figure 3.2(b) The block diagram of Field Emission Scanning Electron Microscope.....	10
Figure 3.3 Block diagram of UV-Visible spectrophotometer.....	11
Figure 3.4 Block diagram of FTIR.....	12
Figure 3.5 Time vs Voltage.....	13
Figure 3.5.1 C-V measurement setup and typical C-V plot (high frequency) for p-type silicon substrate.....	14
Figure.4.1 XRD pattern (a) ZrO ₂ thin film room temperature and (b) ZrO ₂ thin film annealed at 500 °C	16
Figure 4.2(a) and 4.2(b) FESEM image of ZrO ₂ thin film without annealing and annealed at 500 °C.....	17
Fig4.3 FTIR spectra of ZrO ₂ Thin film.....	18
Fig.4.4 (a) wavelength versus transmittance plot of ZrO ₂ thin film and 4.4 (b) $(\alpha h\nu)^2$ versus $h\nu$ curves ZrO ₂ thin film.....	19
Figure 4.5 Capacitance-Voltage plot of ZrO ₂ base MOS	20

Abstract

Zirconium thin films on glass, single-crystal silicon p-type (100), substrates have been prepared from zirconium oxychloride octahydrate and ethanol . The physicochemical processes involved in film formation and the phase composition and properties of the films have been studied. The films prepared on silicon, have a amorphous structure. After annealing at 500 °C the structure changes to tetragonal phase. The resulting ZrO₂ films have bandgap width 4.01 eV, average thickness was 108 nm from UV-visible study. The samples morphological characterizations are done using FESEM. And electrical characterizations are done using Capacitance-Voltage measurements.

Keywords: Zirconium Oxide, thin film, Spin coating, MOS structure, Gate voltage

1. INTRODUCTION

In 1906, L.D Forest invented the first vacuum tube which was used for rectifying, amplifying and switching electrical signals [1]. Vacuum tubes had played an important role in the development of electronics before the advent of semiconductor transistor. In 1947, J. Brattain and W. Bardeen invented the first point contact junction transistor [2,3] and in 1948 W. Shockley proposed bipolar junction transistor (BJT) [4]. In 1951, W. Shockley invented junction field-effect transistor (JFET) [5]. JFET replaced the vacuum tube by a solid state device and found the path for smaller and cheaper electronic devices. In 1958, j. Kilby invented the first integrated circuit and received the Nobel physics prize for his innovative work [6]. For the first time, In 1960, D. Kahng fabricated metal-oxide-semiconductor field effect transistors (MOSFETs) on silicon (Si) substrate using silicon oxide (SiO_2) [7]. MOSFETs rapidly replaced the JFET and had become core of microelectronics. Due to single polarity of MOSFET, it suffered large power dissipation. In 1963, the complementary metal-oxide-semiconductor (CMOS) field effect transistor (FET) which uses both n-type and p-type MOSFETs [8].

Towards the beginning of the 21st century, for the design of the electronic system enormous efforts have been undertaken. For defence, space, automatic control of industrial processes and medical diagnostics, where two parts namely microprocessor and micro sensor actively works during the function of microelectronic device [9-11]. Over the last more than four decades, a successful evolution of Si-based semiconductor technology to increase circuit functionality and performance at lower cost has been continuously driven by scaling down of the metal-oxide-semiconductor field effect transistor (MOSFET). The Semiconductor Industry Association (SIA) has evaluated the goal of industry's products and established a "roadmap" since 1992 to predict the future performance demands and expectations of devices.

1.1.High-k gate dielectrics

Since the inception of the MOSFET in 1960, the gate dielectric material SiO_2 has been used in MOS technology, because of its advantages: (1) the high dielectric breakdown strength ($\geq 10 \text{ MV/cm}$), (2) the electrically stable Si- SiO_2 interface and (3) the thermal stability at high temperature [12]. A SiO_2 layer of 11-15 Å thick (3- 4 monolayers) of SiO_2 creates several problems. First, 11- 15Å thickness is so thin that electrons can directly tunnel through the

SiO₂, resulting in excessively high gate leakage current. High leakage is a great concern, particularly for low power applications, as well as high performance applications. Additionally, SiO₂ thickness uniformity across a wafer (300 mm) becomes even more crucial for such a thin film. Reliability also becomes a huge concern for such a thin SiO₂ dielectric. After so many research, it was found that the materials having high k dielectric can overcome all the problem related to SiO₂.

1.2 Motivation For Zirconium Oxide

Different types of high k materials are taken into consideration such as barium strontium titanate (BST), tantalum oxide (Ta₂O₅), titanium oxide (TiO₂), hafnium oxide (HfO₂), zirconium oxide (ZrO₂), silicon nitride (Si₃N₄) and aluminium oxide (Al₂O₃). Comparison of some important properties of high-k dielectric materials are shown in table 1.

Table.1 Comparison of some important properties of high-k dielectric materials [13-15]

Material	Dielectric constant	energy gap (E _g)	Crystal structure
SiO ₂	3.9	8.9	Amorphous
Al ₂ O ₃	9	8.7	Amorphous
Ta ₂ O ₅	26	4.5	Orthorhombic
TiO ₂	80	3.5	Tetragonal
HfO ₂	25	5.7	Monoclinic, Tetragonal, Cubic
ZrO ₂	25	5.8	Monoclinic, Tetragonal, Cubic

Due to high dielectric constant of BST (~300), it was originally studied for DRAM capacitor application [13]. Later researches discovered that application of BST in MOS capacitors are not thermodynamically stable with silicon because of much higher EOT due to the formation of a relatively thick (~30 Å) Si_xO_y interfacial layer between the BST and silicon substrate. Similarly Ta₂O₅ and TiO₂ are thermodynamically unstable with Si. They interfacial layer

found to be low-k in contact with silicon and result in losing the property of high-k materials [14]. Si_3N_4 has nice interface and good reliability properties [15]. However, relatively low dielectric constant ($k \sim 7.5$) of Si_3N_4 limits its possible application. Al_2O_3 has also similar limitation due to its low dielectric constant ($k \sim 10$). Besides low k, Al_2O_3 well-known interfacial fixed charges consequently results in low carrier mobility in MOSFET applications.

Among the materials hafnium and zirconium based oxides found to be promising candidate since they possess many of the material characteristics required by high-k gate dielectrics. Since ZrO_2 and HfO_2 both have similar structural property, bandgap and dielectric constant, thus we choose ZrO_2 as our base material

1.3 ZrO_2 material properties

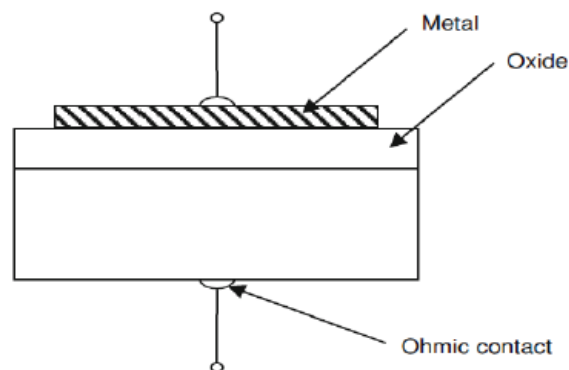
The various material properties of ZrO_2 make an attractive MOS gate dielectric material. ZrO_2 has high dielectric constant of around 25 [16-17] and is stable in contact with Si [18]. It has refractive index ranging from 1.84-2.23 [19] and high density of 5.74 gm/cm^3 , which may help to improve impurity diffusion. As for ZrO_2 's band gap concerned, it is 5.8 eV [20] which is sufficiently high enough for low gate leakage current. It has high melting point nearly 2950 K. Finally, it was reported that ZrO_2 can be etched by diluted hydrofluoric acid (HF) which is used in MOS to remove SiO_2 from Si substrate [21].

Table.2 Material Properties of the ZrO_2 in comparison with SiO_2 [16-21]

Materials	ZrO_2	SiO_2
Dielectric Constant	25	3.9
Bandgap	5.8eV	9eV
Refractive index	1.84-2.23	1.46
Lattice mismatch with Si(100)	2.1%	-
Melting point	2677°C	1600°C
Etchability	HF solution	HF solution
density	5.74 gm/cm ³	2.27gm/cm ³

1.4 The MOS Structure

The important structure of semiconductor devices is metal-oxide-semiconductor (MOS capacitor) which is used in large-scale integration [22]. The MOS capacitor consists of a thin film high k dielectric layer sandwiched between a semiconductor substrate and a metallic field plate. The most common field plate materials and semiconductors are Aluminium and heavily doped polycrystalline Silicon. A second metallic layer present along the back or bottom side of the semiconductor provides an electrical contact to the semiconductor substrate.



[Fig.1.4 Cross-sectional view of a MOS structure]

2. FABRICATION TECHNOLOGY OF ZIRCONIUM OXIDE THIN FILM

Thin film is preferred in the field of microelectronics in which conductive, resistive, insulating films are deposited or sputtered on substrate. Generally, a thin film is layer of material ranging from some nanometer to several micrometer in thickness. Electronic semiconductor devices and optical coatings are the main application of thin films.

In recent years, several attempts have been undertaken for the fabrication of ZrO_2 thin films. These methods are broadly classified into thermal evaporation, Sputtering, Pulsed laser deposition (PLD), Chemical vapour deposition (CVD) and Wet chemical method.

Generally, wet chemical method is called non-vacuum technique and physical method is called vacuum technique. In wet chemical method at least one of the precursors is in liquid phase. Advantages of wet chemical method

- Low cost
- Easily handle
- Less time required
- Less power consumption
- Low temperature deposition

Some examples of chemical methods are

- Spin coating
- Dip coating
- Spray pyrolysis

2.1 Spin coating:

Spin coating is a non vacuum technique used to deposit uniform thin films to flat substrates. A little amount of coating material is put on the centre of the substrate. The substrate is then rotated in order to spread the coating material by centrifugal force. Spin coating is a fast and easy method to generate thin and homogeneous films.

Advantages of spin coating technique:

- Film thickness is changed by changing spin speed
- It produces uniform coating film

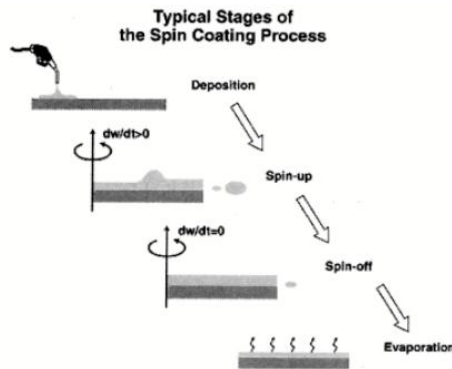


[Figure 2.1 .steps of spin coating methods [23]]

2.2 Thermal evaporation:

Thermal evaporation is a vacuum technique of physical vapor deposition. In this technique, inside the high vacuum chamber a solid material is heated to a high temperature to generate vapour pressure. These vapour are allowed to reach the substrate without reacting or scattering with other atoms in the chamber and reduce the impurities from the residual gas in vacuum chamber. Thermal evaporation depends on parameter like substrate-source distance, substrate temperature, rate of heating, flow rate of gas, working pressure

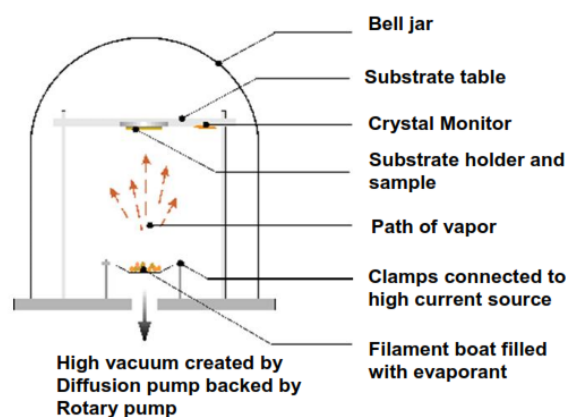


[Figure 2.2 .Block diagram of thermal evaporation system]

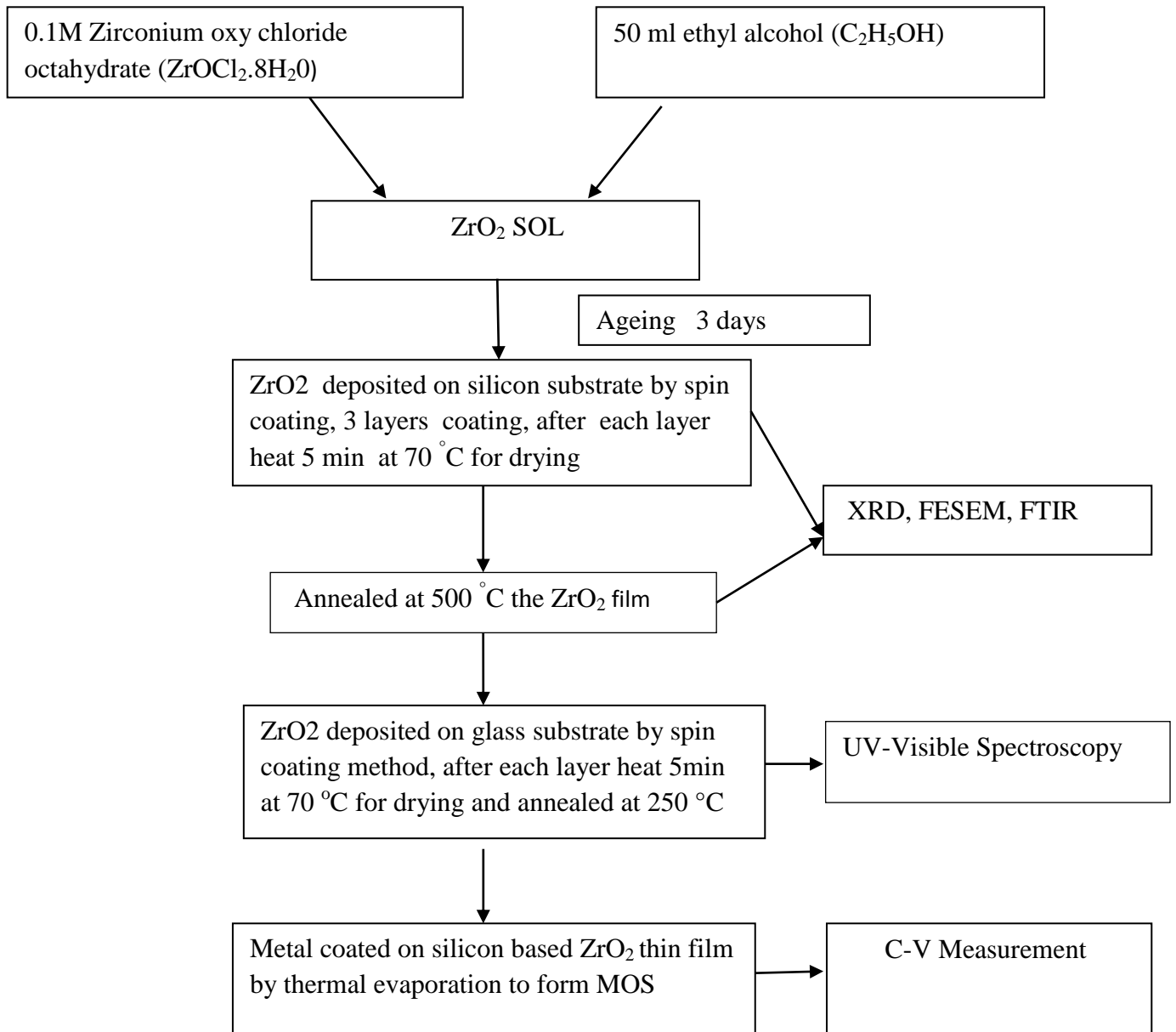
2.3 EXPERIMENTAL:

In the experiment, substrates were taken as Si (100) and glass slides. The substrates were dipped in solution (mixture of hydrogen peroxide and sulfuric acid in 1:1), and rinsed with deionised water. The substrate was heated at 70 °C for 5 min followed by ethanol rinse. The

ZrO₂ sol was prepared by taking 0.1 mol of ZrOCl₂.8H₂O and 50 mL of ethanol as a solvent and the sol was aged at room temperature for 3 days. The deposition of the films on the substrates was done by spin coating at 3000 rpm for 30 seconds. The films were dried at 70°C for 5 min, then annealing to 500 °C at a rate of 10 °C/min and held there for 3 min.

To study capacitance–voltage measurements of Zirconium oxide thin film prepared by spin coating method, zirconium oxide based MOS (metal oxide semiconductor) device was prepared by thermal evaporation method. In the MOS device the top contact was done by local metallization of aluminum using mask and the bottom contact was done globally by aluminium metal. The Capacitance-Voltage measurements was done by Agilent E4980A precision LCR meter .The structural properties of the prepared ZrO₂ thin film by spin coating was investigated by X-ray diffraction system (Rigaku Corporation manufactured Ultima IV). The optical properties were studied by UV- Visible Spectrophotometer. The experimental details was represented by the flowchart given below,

Flow chart of the Experimental work



3.CHARACTERIZATION TECHNIQUES

It is necessary to study the structural, compositional, morphological and other properties for sample characterization. To study the structural details about the samples x-ray diffraction, for morphological Field emission electron microscope, for optical properties UV-Visible spectroscopy and Fourier transform infrared spectroscopy and electrical properties Capacitance-Voltage measurements were performed.

3.1 X-Ray diffraction

This is a technique to study structural details of the samples. By this technique size and shape of the crystal, the average atomic spacing, orientation of the single and ploy crystal are determined.

The Bragg's law describing relationship a beam of X-ray having particular wavelength diffracts at certain angle from a crystalline surface defined by equation,

$$n\lambda = 2d \sin\theta \dots\dots\dots [3.1]$$

λ = X-ray wavelength

d = distance between lattice planes

θ = angle of incidence with lattice plane

n = integer

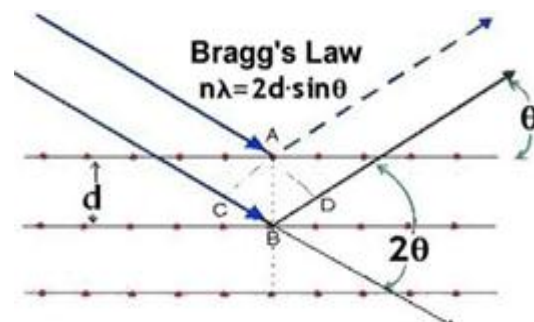


[Figure 3.1 .X-Ray Diffraction condition]

When X-ray passes through the matter it interacts with the atom or electron inside the materials. The light deflected from each element will be different and corresponding intensity also different. When the intensity of those deflected light is plotted with respect to the angle of diffraction, different peaks are obtained. From those peaks the structure of the material and also size of the crystalline can be detected from the peak width. If width of the peak increases then the crystalline size of the sample decreases. This indicates that peak width is inversely proportional to crystalline size. Peak width also depends on the angle of deflection 2θ , at larger deflecting angles the broadening of crystalline size is more.

3.2 Field emission scanning electron microscope (FESEM):

FESEM provides clear and less distorted images and also gives 3 to 6 times more resolution than SEM. Good quality and low voltage images are obtained with less electrical charging of samples by FESEM. The need for conducting coatings on insulating materials is virtually eliminated.

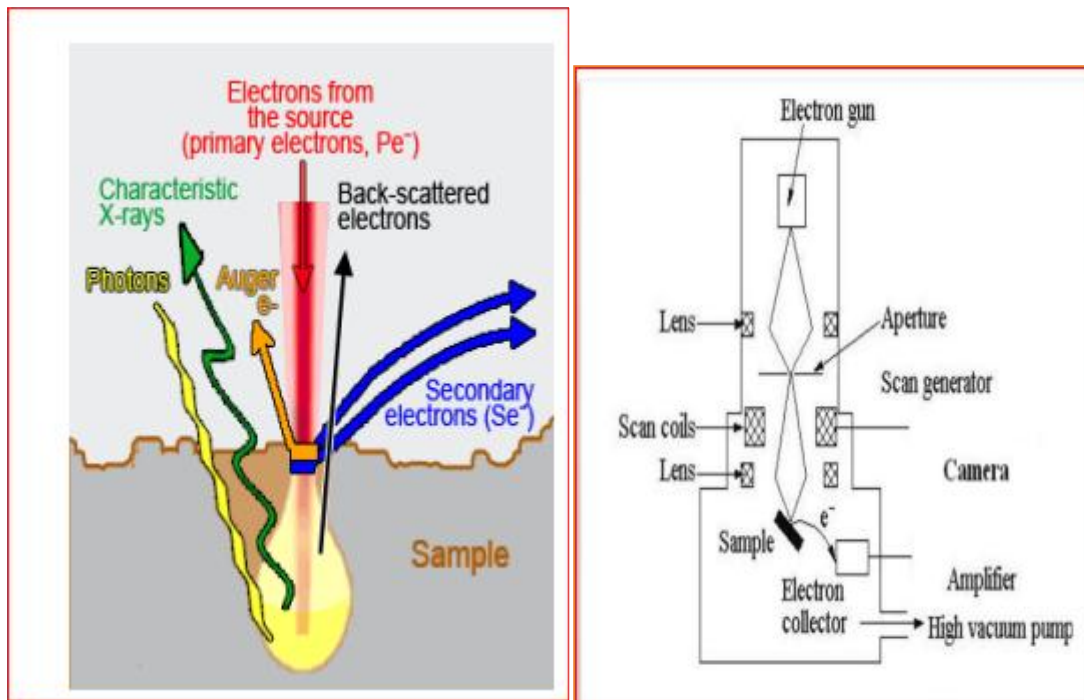


[Figure 3.2(a) .The emission of secondary Electrons from the specimen [24]]

[Figure 3.2(b) the block diagram of Field Emission Scanning Electron Microscope [24]]

3.3 UV-Visible Spectroscopy:

Ultraviolet–Visible spectroscopy refers to absorption, reflectance or transmittance spectroscopy in the ultraviolet-visible spectral region [25]. The absorption or reflectance in the visible range directly affects the chemicals color. This technique is opposite to fluorescence spectroscopy. In fluorescence the transitions takes place from the excited state to the ground state while in absorption transitions occurs from the ground state to the excited state

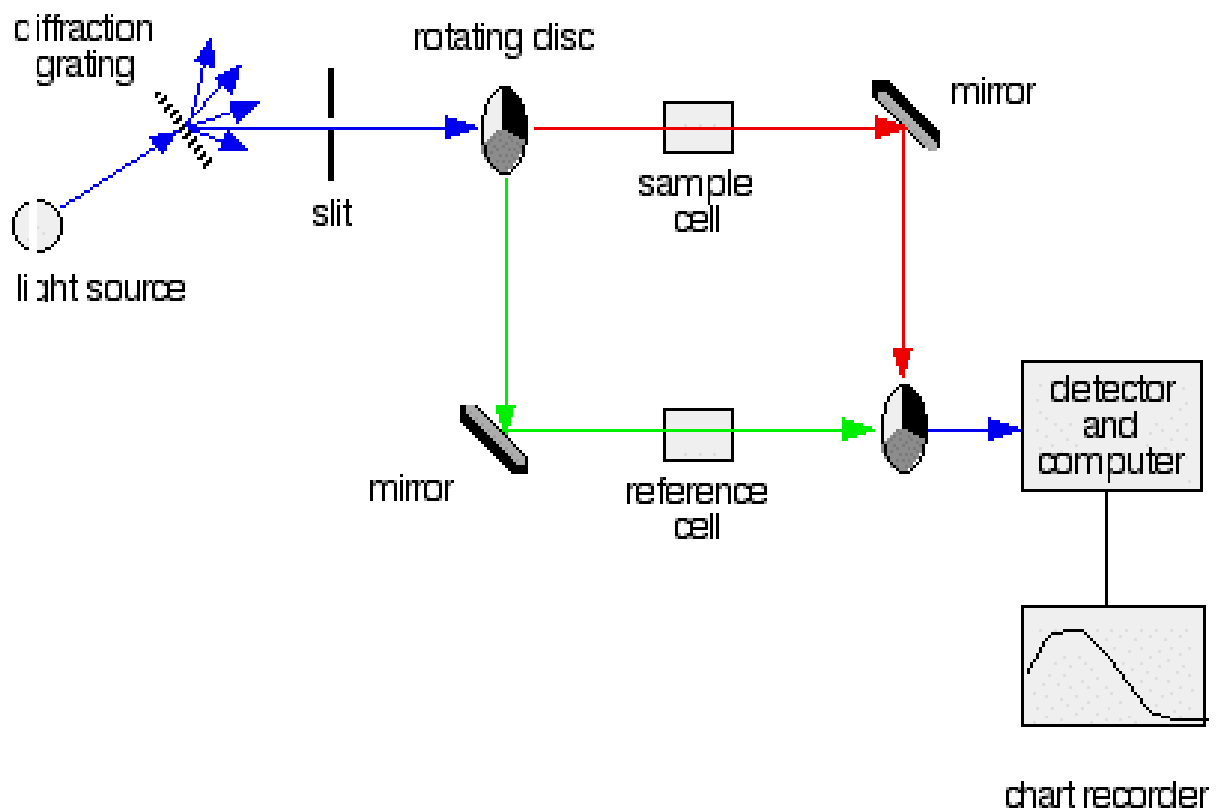


[Figure 3.3 Block diagram of UV-Visible Spectrophotometer [26]]

By using UV-Visible Spectroscopy, we can calculate the band gap of thin film using relation

$$(\alpha h\nu)^{1/n} = B(h\nu - E_g)$$

B: a constant related to a transition probability

E_g : band gap

N: an index characterizing the transition step

$n=2$ is an indirect transition step

$n= \frac{1}{2}$ is a direct allowed transition step

3.4 Fourier transform infrared spectroscopy:

All the IR wavelengths are measured simultaneously by the spectrometer which produces a full spectrum. Based on the use of interferometer called as an optical modulator, the radiation emitted by the IR-source is modulated, which produces an interferogram containing all the infrared frequencies encoded in it. An optical Fourier transform on the IR radiation emitted by the IR source is performed by the interferometer.

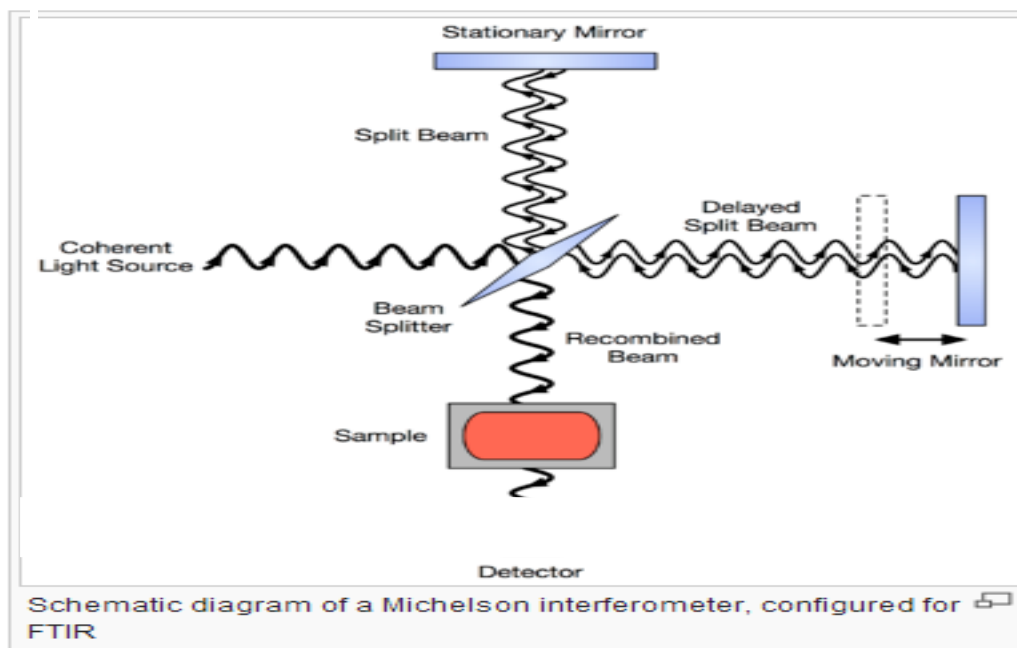


[Figure 3.4. Block diagram of FTIR [27]]

3.5 Capacitance-Voltage measurement (C-V measurement):

The single most important measurement in Metal-Oxide-Semiconductor (MOS) work is a plot of the capacitance of a MOS structure as a function of its dc gate bias. This is known as a C-V (capacitance-voltage) plot. The Capacitance-Voltage (C-V) technique is the most

commonly used tool for the electrical characterization of high-k gate dielectrics and metal gate electrodes. Many important electrical properties of high-k gate dielectrics, including dielectric constant, EOT, flat band voltage, fixed charges, bulk charges, and interface state density derived from the C-V measurement. The work function of the metal gate electrodes can also be calculated from the C-V measurement by plotting the flatband voltage and EOT of MOS capacitors with various thicknesses. The inversion capacitance can provide the information of the Si substrate doping concentration.

During the C-V measurement, a small sinusoidal AC drive signal is superimposed on a linear DC voltage ramp to sweep over the bias range from accumulation region to inversion region shown in the fig 4.5. The frequency of this sinusoidal ac voltage can be varied from 20 Hz to 1MHz. A frequency (above 100 kHz) is commonly considered as the high frequency.

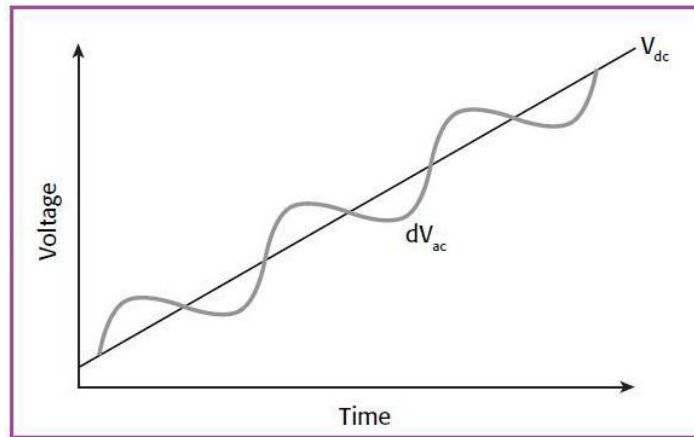


[Figure 3.5 time vs voltage]

3.5.1 High frequency C-V plots

Capacitance meters measure capacitance by applying a small (\sim mV) ac voltage on top of the dc bias and measuring the reactive component of the resulting current. As indicated in Fig. 3.5.1, applying negative gate voltage, In p-type silicon one can measure the dielectric constant of the film from the accumulation region. When gate voltage becomes more than flat band voltage, this creates a capacitor in series with oxide capacitance. When dc voltage exceeds the threshold voltage V_T , inversion of charge occurs. Then if the dc voltage is slowly increased further, the inversion layer increases its charge to balance the gate and the depletion layer does not widen further. Since the depletion-layer width has reached a maximum, the total ac capacitance is pegged at its minimum

Accumulation region

When the $-Ve$ voltage applied to the gate, accumulation occurs. The $-ve$ charge on the gate attracts the holes from the semiconductor.

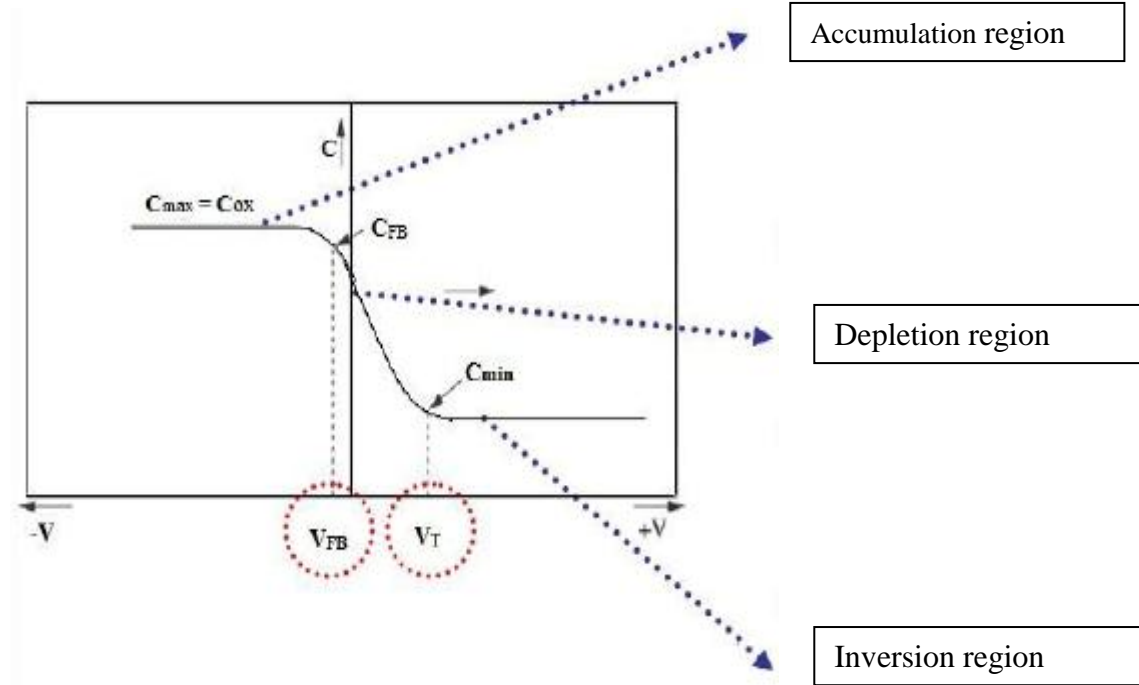


[Figure 3.5.1 C-V measurement setup and typical C-V plot (high frequency) for p-type silicon substrate]

Depletion Region

Depletion occurs at positive voltage. The $+ve$ charge on the gate pushes the holes into the substrate and causing depletion at the oxide-semiconductor interface.

Inversion Region

Inversion takes place at threshold voltage. The inversion layer is due to minority carriers of semiconductor substrate.

3.5.2. Extracting the Flatband capacitance and Flatband voltage

When certain voltage is applied, the flatband voltage (V_{FB}) results in the disappearance of bending of band. As this point, known as the flatband condition, the semiconductor band is said to become flat. Flat band voltage and its shift are widely used to extract other device parameters, such as oxide charges [28].

The C_{FB} is derived using the equation 3.5.2(a) and 3.5.2(b). The value of V_{FB} can be derived from the corresponding C-V curve data [29].

Equation 4.5.2(b) calculates the Debye length parameter (λ) that is used in equation 3.5.2 (a) [30].

$$C_{FB} = \frac{C_{ox}\epsilon_s A / (1 \times 10^{-4})(\lambda)}{(1 \times 10^{-12})(C_{ox}) + \epsilon_s A / (1 \times 10^{-4})(\lambda)} \dots\dots\dots [3.5.2(a)]$$

Here C_{FB} is the flatband capacitance (pF)

C_{ox} is the oxide capacitance (pF)

ϵ_s is the permittivity of the substrate material (F/cm),

A is the gate area (cm^{-2})

λ is the extreme Debye length, calculated from:

$$\lambda = \left(\frac{\epsilon_s kT}{q^2 Na} \right)^{\frac{1}{2}} \dots\dots\dots [3.5.2(b)]$$

Where kT is the thermal energy

q is the electron charge

N_a is doping concentration.

3.5.3. Extraction of Oxide charge

The effective oxide charge (Q_{EFF}) is the sum of the oxide fixed charge (Q_F), the mobile charge (Q_M), and the oxide trapped charge (Q_{OT})

The calculation of Q_{EFF} is given by the equation [3.5.3 (a)] [29,30],

$$V_{FB} - W_{MS} = -\frac{Q_{EFF}}{C_{OX}} \dots\dots\dots [3.5.3 (a)]$$

Where V_{FB} is the flatband voltage (V)

W_{MS} is the metal-semiconductor work function

and C_{ox} is the oxide capacitance.

4. RESULTS AND DISCUSSION:

4.1 X-Ray diffraction:

Figure 4.1(a) shows the XRD pattern of multilayer ZrO_2 thin film room temperature and Fig 4.1(b) shows the ZrO_2 film deposited on Si (100) substrate after annealing at 500 °C. Fig 4.1(a) show that the ZrO_2 film has amorphous structure with one peak (100) corresponding to the peak of the silicon substrate. After annealed at 500 °C ,two peak in addition to Si peak as shown in fig(b). These are (200) and (311) peak at an angle 33.08° and 61.75°. The film transition from amorphous to crystalline structure at 500 °C which is tetragonal in structure [31].

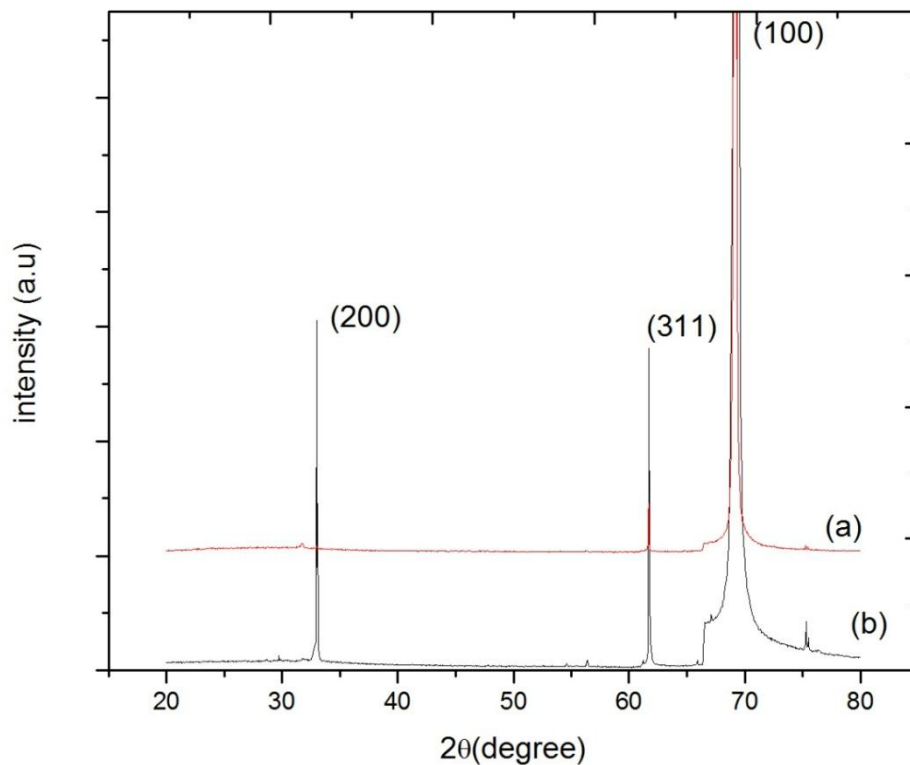


[Figure.4.1 XRD pattern (a) ZrO_2 thin film room temperature and (b) ZrO_2 thin film annealed at 500 °C]

4.2 Field emission scanning electron microscope(FESEM):

Figure 4.2(a) shows the FESEM micrographs of the ZrO_2 thin film without annealing and with annealing is shown in the figure 4.2(b). The thin films of ZrO_2 shows a uniform and less crack surface before annealing. After annealing the cracks are slightly reduced as compared to non-annealing process.

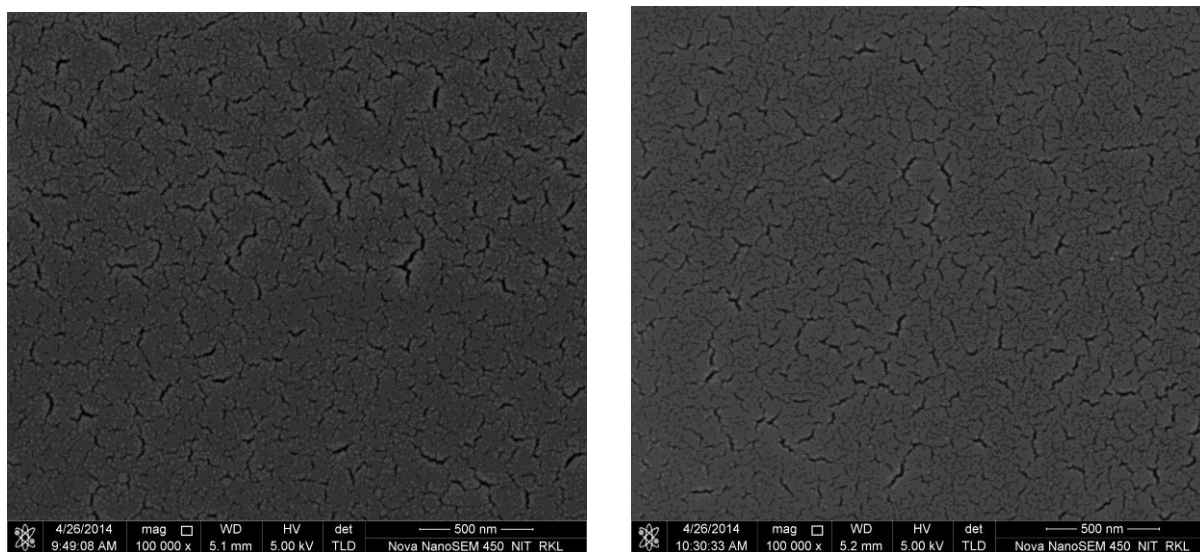


[Figure .4.2(a) and 4.2(b) FESEM image of ZrO_2 thin film without annealing and annealed at 500 °C]

4.3 Fourier transform infrared spectroscopy (FTIR):

Figure 4.3 shows the FTIR spectra of ZrO_2 thin films deposited by spin coating technique. The band at 609 cm^{-1} indicates vibration of Zr-O bond. Dhar [32] investigated ZrO_2 thin films deposited by MOCVD technique using beta ketoesterate complex and obtained similar type of microstructure. The band at 1098 cm^{-1} corresponds to the vibration of the Si-O bond.

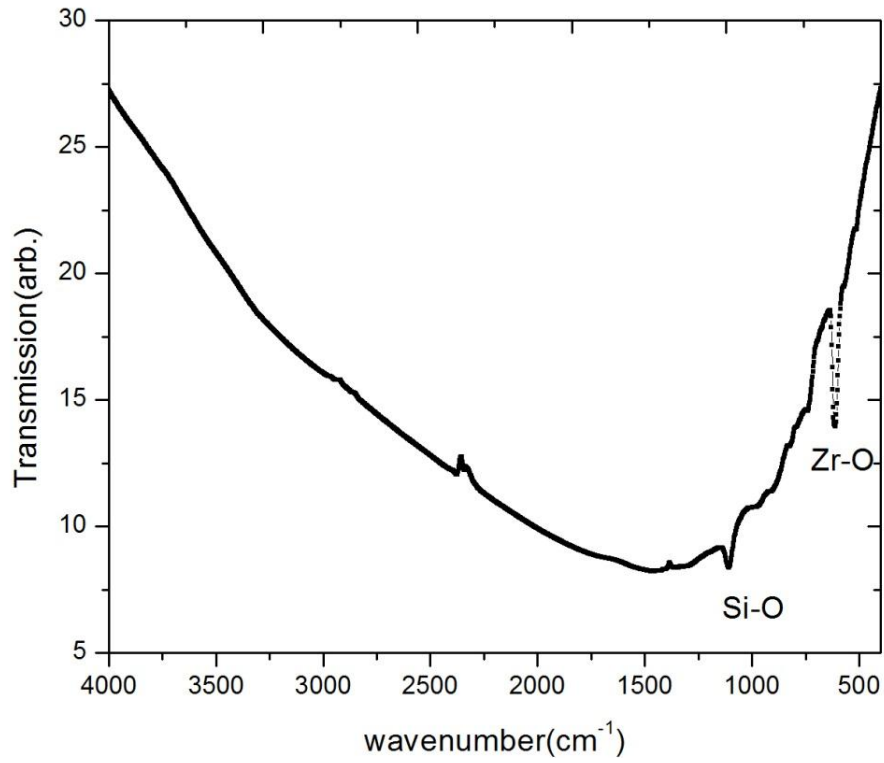


[Fig 4.3 FTIR spectra of ZrO₂ Thin film]

4.4 UV–visible spectroscopy (UV-Vis):

The wavelength versus transmission plot shows the transmittance spectra of ZrO₂ thin film. The optical energy gap of ZrO₂ thin film is calculated by using the Tauc method [33]. The energy gap is calculated using the relation

$$(\alpha h\nu)^2 = B(h\nu - E_g)$$

Where $h\nu$ is the incident photon energy and B is a constant

The $(\alpha h\nu)^2$ versus $h\nu$ curves for ZrO_2 thin film are shown in Fig 4.4 (b). The band gap for the ZrO_2 thin film is found to be 4.01 eV. The decrease of E_g may be assumed to the adjustment of atoms to more stable positions by annealing [34].

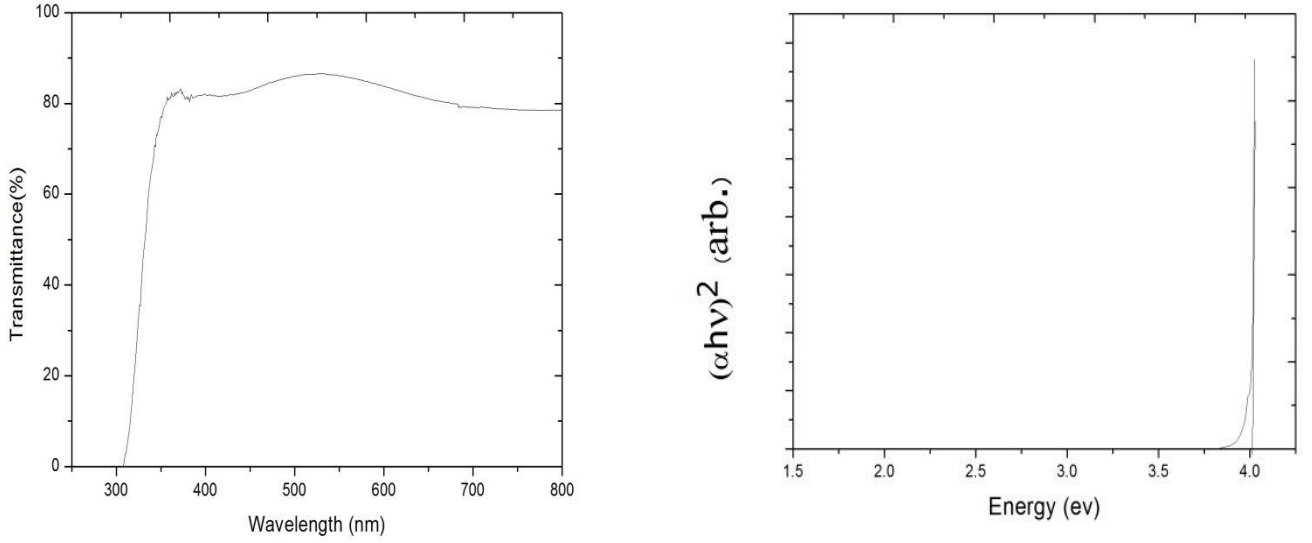


[Fig.4.4 (a) wavelength versus transmittance plot of ZrO_2 thin film and 4.4 (b) $(\alpha h\nu)^2$ versus $h\nu$ curves ZrO_2 thin film]

Fig. 4.4 (a) shows the transmittance spectrum of the zirconium oxide films. There are two minima at 423 nm and 688 nm,. The thickness of zirconium oxide films is calculated with using the formula [35]:

$$d = \frac{1}{2n\left(\frac{1}{\lambda_1} - \frac{1}{\lambda_2}\right)}$$

Where d is the film thickness

n is the refractive index ($n = 3.9$)

λ_1 and λ_2 are the wavelength of adjacent peaks in the transmittance spectrum

so the film thickness $d = 108$ nm.

4.5 Capacitance-Voltage measurement(C-V):

C-V measurements were carried out by using Agilent E4980 precision LCR meter and plotted in Fig. 5.5. Three regions of the C-V graph, namely accumulation, depletion and inversion, formed due to variation in carrier concentrations at the interface with bias voltage, are distinctly visible. The maximum capacitance in the accumulation region was found to be 1130.28 pF.

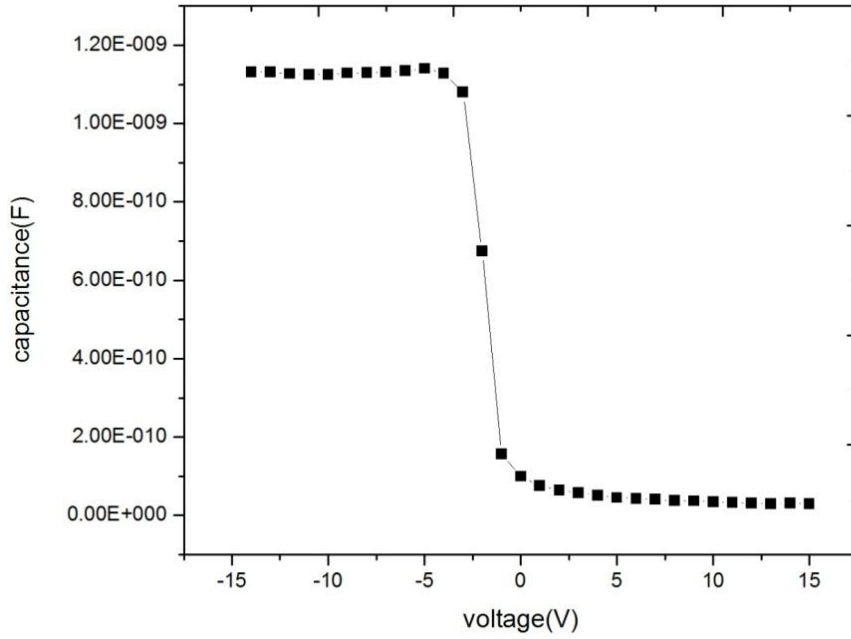


[Figure 4.5.Capacitance-Voltage plot of ZrO₂ base MOS]

By using equation no 3.5.2 (a) the flat band capacitance was found as 556 pF and the corresponding flat band voltage was -1.67 V. Using equation 3.5.3(a) the effective oxide charge was 109.92×10^{-9} C and the effective oxide charge density was found to be 6.87×10^{11} ions/cm². The dielectric constant of the ZrO₂ thin film was estimated to be 17 from the accumulation region of the C-V diagram.

6. CONCLUSION:

Zirconium Oxide thin films were prepared on p-type silicon and glass substrate using spin coating deposition method. It was observed from the X-ray diffraction that Zirconium oxide film prepared at ambient temperature shows amorphous structure and changes to crystalline with annealed at 500 °C. The Zr-O bond and Si-O which are at the wavelengths 609 cm^{-1} and 1098 cm^{-1} respectively was seen from the FTIR study. From UV-visible study the band gap of the Zirconium oxide film was found to be 4.01 eV and the average thickness of the film was found as 108 nm. The oxide capacitance, flat band capacitance, flat band voltage, effective oxide charge and effective oxide charge density were found to be 1130.32 pF, 556 pF, -1.67 V, $109.92 \times 10^{-9}\text{ C}$ and $6.87 \times 10^{11}\text{ ions/cm}^2$ respectively. The dielectric constant of the ZrO_2 thin film was estimated to be 17 from the accumulation region of C-V diagram.

References

- [1] Forest L D, Oscillation responsive device, U.S. Patent No. 8724637, filed Jan. 18 1906, issued June 26 1906.
- [2] Bardeen J, Surface states and rectification at a metal semi-conductor contact, Phys. Rev., **72**(10), (1947) 717.
- [3] Brattain W H, Evidence for surface states on semiconductors from change in contact Potential on illumination, Phys. Rev., **72**(4), (1947) 345.
- [4] Shockley W, Semiconductor amplifier, U.S. Patent No. 2502488, filed Sept. 24 1948, Issued April 4 1950.
- [5] Shockley W, Sparks M, and Teal G K, p-n junction transistors, Phys. Rev., **83**(1), (1951), 151.
- [6] http://www.nobelprize.org/nobel_prizes/physics/laureates/2000.
- [7] Kahng D and Atalla M M, Silicon-silicon dioxide surface device, IRE-AIEE Solid-state Device Res. Conf., (Carnegie Institute of Technology, Pittsburgh, PA), (1960).
- [8] Wanless F, and Sah C, Nanowatt logic using field effect metal-oxide-semiconductor Triodes, IEEE ISSCC Tech. Dig., (1963), 32.
- [9] N.A Weir, D.P. Sierra, J.f. Jones, "A review of research in the field of nanorobotics". S. Department of energy, (2005)
- [10] L. Dong, X. Tao, L. Zhang, X. Zhang, B.J. Nelson, Nano Letters, **7** (2007) 58.
- [11] R. McGowen, C.A. Poirier, C. Bostak, J. Ignowski, M. Millican, W.H. Parks, S. Naffziger, IEEE J. Solid state circuits, **41**(006) 229
- [12] L D Forest, Oscillation responsive device, U.S. Patent No. 8724637, filed Jan. 18 1906, issued June 26 1906.
- [13] T. Chen, D. Hadad, V. Balu, B. Jiang, S. Kuah, P.C. McIntyre, S.R. Summerfelt, J.M. Anthony, and J.C. Lee, Ir-Electroded BST Thin Film Capacitors for 1 Gigabit DRAM Application, International Electron Devices Meeting, IEDM Technical Digest, (1996), 679.

- [14] H. F. Luan, S. Lee, S. Song, Y. Mao, Y. Senaki, D. Roberts, and D. L. Kwong, "High quality Ta₂O₅ gate dielectrics with $T_{ox} < 10 \text{ \AA}$ ", Tech. Dig. IEDM, (1999), 141.
- [15] S. C. Song, H. F. Luan, M. Gardner, J. Fulford, M. Allen, and D. L. Kwong, "Ultra Thin (<20 Å) CVD Si₃N₄ Gate Dielectric for Deep-Sub-Micron CMOS Devices", IEDM Tech. Dig., (1998), 37
- [16] M. Balog, M. Schieber, M. Michman, and S. Patai, "The chemical vapour Deposition and characterization of ZrO₂ films from organ metallic compounds," Thin Solid Films, vol. 47, 1977, 109.
- [17] C.S. Hwang and H.J. Kim, "Deposition and characterization of ZrO₂ thin films On silicon substrate by MOCVD," Journal of Materials Research, vol. 8, no. 6, 1993, 1361.
- [18] K.J. Hubbard and D.G Schlom, "Thermodynamic stability of binary oxides in Contact with silicon," Journal of Materials Research, vol. 11, no. 11, 1996, p. 2757,
- [19] P.J. Martin, R.P. Netterfield, and W.G. Sainty, "Modification of the optical and Structural properties of dielectric ZrO₂ films by ion-assisted deposition," Journal Of Applied Physics, vol. 55, no. 1, 1984, p. 235.
- [20] J. Robertson, E. Riassi, J.-P. Maria, and A.I. Kingon, "Band alignments of high k Dielectrics on Si and Pt," Materials Research Society Symposium Proceedings Series, vol. 592, 1999.
- [21] C.S. Hwang and H.J. Kim, "Deposition and characterization of ZrO₂ thin films on silicon substrate by MOCVD," Journal of Materials Research, vol. 8, no. 6, 1993 p. 1361.
- [22] The MOS structure, Transport in Metal-Oxide-Semiconductor Structures, Engineering materials, DOI: 10.1007/978-3-642-16304-3_2
- [23] Niranjana Sahu*, B Parija and S Panigrahi, Department of physics, National Institute of Technology, Rourkela – 769008, Orissa, India, Indian J. Phys. 83(4) 493-502 (2009)
- [24] [http://shodhganga.inflibnet.ac.in/bitstream/10603/8936/10/10_chapter 202.pdf](http://shodhganga.inflibnet.ac.in/bitstream/10603/8936/10/10_chapter%202.pdf)
- [25] Skoog; et al. (2007). Principles of Instrumental Analysis (6th ed.). Belmont, CA: Thomson Brooks/Cole. pp. 169–173. ISBN 9780495012016.

- [26] <http://www.chemguide.co.uk/analysis/uvvisible/spectrometer.html>
- [27] http://en.wikipedia.org/wiki/Fourier_transform_infrared_spectroscopy
- [28] D. G. Ong, Modern MOS Technology: Processes, Devices, and Design, McGraw-Hill,(1986).
- [29] E. H. Nicollian and J. R. Brews, MOS Physics and Technology, Wiley, New York 1982).
- [30] S. M. Sze, Physics of Semiconductor Devices, 2nd edition, Wiley, New York (1985)
- [31] State Key Laboratory of Solid Lubrication, Lanzhou Institute of Chemical Physics, Chinese Academy of Sciences, Lanzhou 730000, People's Republic of China
- [32] S. Dhar and M. S. Dharmaparakash, "MOCVD of ZrO₂ Films from Bis(t-Butyl-3-oxobutanoato) Zirconium (IV): Some Theoretical (Thermodynamics) and Experimental aspects," Material Science, Vol. 31, 2008, pp. 67-72.
- [33]. J. Tauc, R. Grigorovici, A. Vancu, Phys. Status Solidi 15, (1966), p 627.
- [34] A.F. Khan, M. Mehmood, A.M. Rana, M.T. Bhatti, A. Mahmood, Chin. Phys. Lett. 26 (2009) 077803
- [35] J.I. Pankov, Optical Processes in Semiconductors, Dover, New York, 197 (Chapter 4).